Differential Effects of Acetylcholine and Glutamate Blockade on the Spatiotemporal Dynamics of Retinal Waves

Evelyne Sernagor,[1] Stephen J. Eglen,[2] and Michael J. O'Donovan[3]

[1]*Department of Child Health, The Medical School, University of Newcastle upon Tyne, Newcastle upon Tyne, NE2 4HH, United Kingdom,* [2]*Institute for Adaptive and Neural Computation, Division of Informatics, University of Edinburgh, Edinburgh, EH8 9LW, United Kingdom, and* [3]*Laboratory of Neural Control, National Institute of Neurological Diseases and Stroke, National Institutes of Health, Bethesda, Maryland 20892*

In the immature vertebrate retina, neighboring ganglion cells express spontaneous bursting activity (SBA), resulting in propagating waves. Previous studies suggest that the spontaneous bursting activity, asynchronous between the two eyes, controls the refinement of retinal ganglion cell projections to central visual targets. To understand how the patterns encoded within the waves contribute to the refinement of connections in the visual system, it is necessary to understand how wave propagation is regulated. We have used video-rate calcium imaging of spontaneous bursting activity in chick embryonic retinal ganglion cells to show how glutamatergic and cholinergic connections, two major excitatory synaptic drives involved in spontaneous bursting activity, contribute differentially to the spatiotemporal patterning of the waves. During partial blockade of cholinergic connections, cellular recruitment declines, leading to spatially more restricted waves. The velocity of wave propagation decreases during partial blockade of glutamatergic connections, but cellular recruitment remains substantially higher than during cholinergic blockade, thereby altering correlations in the activity of neighboring and distant ganglion cells. These findings show that cholinergic and glutamatergic connections exert different influences on the spatial and temporal properties of the waves, raising the possibility that they may play distinct roles during visual development.

Key words: retinal waves; spatiotemporal properties; chick embryo; glutamate; acetylcholine; visual system development; calcium imaging; retinal ganglion cells

Long before birth, vertebrate retinal ganglion cells fire in spontaneous bursts of action potentials (Masland, 1977; Maffei and Galli-Resta, 1990; Sernagor and Grzywacz, 1995; Wong, 1999). This spontaneous bursting activity (SBA) is correlated between neighboring cells, spreading as waves across the developing retina (Meister et al., 1991; Wong et al., 1993, 1995, 1998; Catsicas et al., 1998; Wong, 1999). Previous studies suggest that SBA, asynchronous between the two eyes, controls the segregation of ganglion cell central projections into eye-specific layers in mammals (Katz and Shatz, 1996; Shatz, 1996; Weliky and Katz, 1997; Penn et al., 1998; Crair, 1999; Wong, 1999) and the removal of aberrantly placed arbors and ipsilateral connections in the chick (Kobayashi et al., 1990; Pequignot and Clark, 1992a,b). An important conceptual distinction for understanding the role of retinal SBA in guiding the development of connections in the visual system is whether the spontaneous activity is permissive or instructive (Crair, 1999). If permissive, the formation of connections would depend only on the presence of SBA. If instructive, then the specific patterns encoded within the waves would be necessary for shaping the appropriate connections. Although it is believed that patterns of retinal SBA are indeed important for refining the arrangement of neural connections, very little experimental evidence supports that view. To understand how the patterns encoded within the waves contribute to the refinement of connections in the visual system, it is first necessary to understand how wave propagation is regulated.

Both cholinergic nicotinic (Feller et al., 1996; Sernagor and Grzywacz, 1996, 1999; Catsicas et al., 1998) and glutamatergic (Miller et al., 1998; Wong et al., 1998; Sernagor and Grzywacz, 1999) synaptic transmissions are known to participate in wave/SBA generation in vertebrates (Wong, 1999), but it is not known whether, or how, these connections contribute to wave propagation patterns. A theoretical study argues that cholinergic lateral connections are sufficient for wave propagation (Feller et al., 1997), but no experiments have established this point. In the present study, we have used partial cholinergic and glutamatergic blockade—to perturb the waves without completely abolishing them—to dissociate the relative contributions of glutamatergic and cholinergic inputs to wave propagation and recruitment. Our study was performed in embryonic day 14–15 (E14–15) chick

Received Sept. 21, 1999; revised Nov. 10, 1999; accepted Nov. 15, 1999.

This work was supported by a NATO Collaborative Research grant to E.S. and M.O.D. and by a Wellcome Trust Mathematical Biology Fellowship to S.E. We thank Peter Wenner for his help with the experimental setup and Daniel Osorio and Julian Budd for their helpful comments on this manuscript.

Correspondence should be addressed to Evelyne Sernagor, Department of Child Health, The Medical School, Framlington Place, Newcastle upon Tyne, NE2 4HH, UK. E-mail: Evelyne.Sernagor@ncl.ac.uk.

This article is published in *The Journal of Neuroscience*, Rapid Communications Section, which publishes brief, peer-reviewed papers online, not in print. Rapid Communications are posted online approximately one month earlier than they would appear if printed. They are listed in the Table of Contents of the next open issue of JNeurosci. Cite this article as: JNeurosci, 2000, 20:RC56 (1–6). The publication date is the date of posting online at www.jneurosci.org.

http://www.jneurosci.org/cgi/content/full/3876

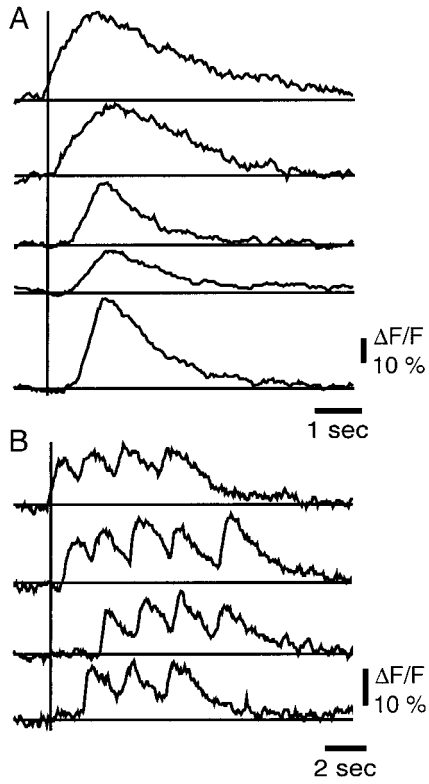

Figure 1. Calcium transients generated in individual ganglion cells during a single wave. *A*, Transients from five ganglion cells in the same retina. There is great variability in signal amplitude, rate of rise, and duration of the calcium transients. The *vertical line* indicates the onset time of the top transient, showing that cells do not become simultaneously active. *B*, Transients generated in four cells during a wave recorded in another retina. Most cells generated multicyclical calcium transients in this retina. $\Delta F/F$, Change in fluorescence.

retinas, when synapse formation is in advanced stages (Hughes and LaVelle, 1974), both acetylcholine (ACh) and glutamate contribute to the waves (Sernagor and O'Donovan, 1997), and retinal projections undergo refinement in the optic tectum (Mey and Thanos, 1992; Wong, 1999).

MATERIALS AND METHODS

Surgical procedure, dye labeling of the retina, and drug application. Chick eye cups were isolated at 12°C (after egg cooling, decapitation, pithing, enucleation, and eye hemisection). Retinal ganglion cells were retrogradely loaded from the optic nerve with a solution of calcium green dextran as described elsewhere (O'Donovan et al., 1993). The eye cup was perfused with oxygenated Tyrode's solution (O'Donovan and Landmesser, 1987) for 15–24 hr at 18°C to allow sufficient time for dye transport and loading of cell somata. The retina was isolated from the eye cup and transferred, ganglion cell layer facing down, onto the stage of an inverted microscope (Nikon, Diaphot). The chamber was continuously perfused (5–10 ml/sec) with oxygenated solution.

The pharmacological agents (Sigma, St. Louis, MO) were bath-applied through the perfusate (one drug per retina). For glutamatergic blockade, we used kynurenic acid, a broad-spectrum antagonist ($n = 1$ retina), 6-cyano-7-nitroquinoxaline-2,3-dione (CNQX), an AMPA/kainate antagonist ($n = 6$), and D(−)-2-amino-5-phosphonopentanoic acid (D-AP-5) ($n = 3$), an NMDA antagonist. The nicotinic antagonists curare ($n = 1$) and mecamylamine ($n = 5$) were used to block cholinergic receptors. The concentration of the drugs was typically 0.5–5 μM, although sometimes doses up to 20 μM of D-AP-5 were required. We have pooled the results obtained with the various antagonists of each neurotransmitter because their effects were similar.

After the effect of partial cholinergic or glutamatergic blockade was assessed, the concentration of the drug was sometimes increased to verify that the waves had disappeared. Prolonged washout (1 hr) after this procedure led only to poor recovery. The frequency of wave-like activity increased, but other wave parameters did not recover significantly.

Analysis of calcium transients. Ganglion cells labeled with calcium green dextran were viewed at 20× with standard fluorescein filters (480 nm, 510 nm barrier). Fluorescence changes were detected using an intensified CCD camera (Stanford Photonics) and recorded continuously (30 frames/sec) onto video tape. Camera output was also viewed on-line using the image analysis software MetaMorph (Universal Imaging) run on an IBM-compatible computer.

Selected episodes of activity were later transferred from video onto an optical disk (Panasonic TQ-3031F). The fluorescence in selected cells [or regions of interest (ROI)] was measured using MetaMorph by digitizing individual video frames from the disk and then averaging the pixels within each ROI. Cells were selected by the presence of activity in at least one of all waves in the control and drug conditions, which generally involved >90% of the labeled cells within the field of view. Frame-by-frame changes in fluorescence were analyzed using software written for this project. Signals were normalized to the resting level of fluorescence

Table 1. Comparison between changes in wave parameters during glutamatergic and cholinergic blockade

Parameter	Percentage difference from control: Glutamate blockade	Percentage difference from control: ACh blockade	Significance level (p)
Wave frequency (waves/hr)	−41.7 ± 10.3	−54.6 ± 12.7	0.46 (ns)
	n_c 78; n_d 76	n_c 49; n_d 31	
Ca^{2+} transients amplitude ($\Delta F/F$)	−21.6 ± 4.0	−29.8 ± 7.7	0.31 (ns)
	n_c 5,006; n_d 4,789	n_c 2,280; n_d 1,168	
Ca^{2+} transients rate of rise ($\Delta F/F$/sec)	−28.9 ± 4.4	−34.4 ± 5.4	0.45 (ns)
	n_c 5,006; n_d 4,789	n_c 2,280; n_d 1,168	
Wave velocity (μm/sec)	−41.0 ± 6.6	7.7 ± 18.2	0.0074*
	n_c 299; n_d 340	n_c 157; n_d 147	
Cellular recruitment (%)	−17.6 ± 4.3	−45.1 ± 6.7	0.0026*
	n_c 42; n_d 36	n_c 28; n_d 22	

Changes are expressed in percentage difference from control. Parameters were calculated over 11 retinas for glutamate blockade and six retinas for ACh blockade. (Wave velocity could not be computed for one glutamate retina and two ACh retinas.) n_c and n_d indicate the number of data points for control and drug blockade, respectively (number of waves, wave frequency; number of transients, Ca^{2+} transient amplitude and rate of rise; number of cell pairs, wave velocity; number of waves, cellular recruitment). The significance of differences between glutamate and ACh blockade was measured using the two-tailed t test. ns, Not significant. * Significant. $\Delta F/F$, Change in fluorescence.

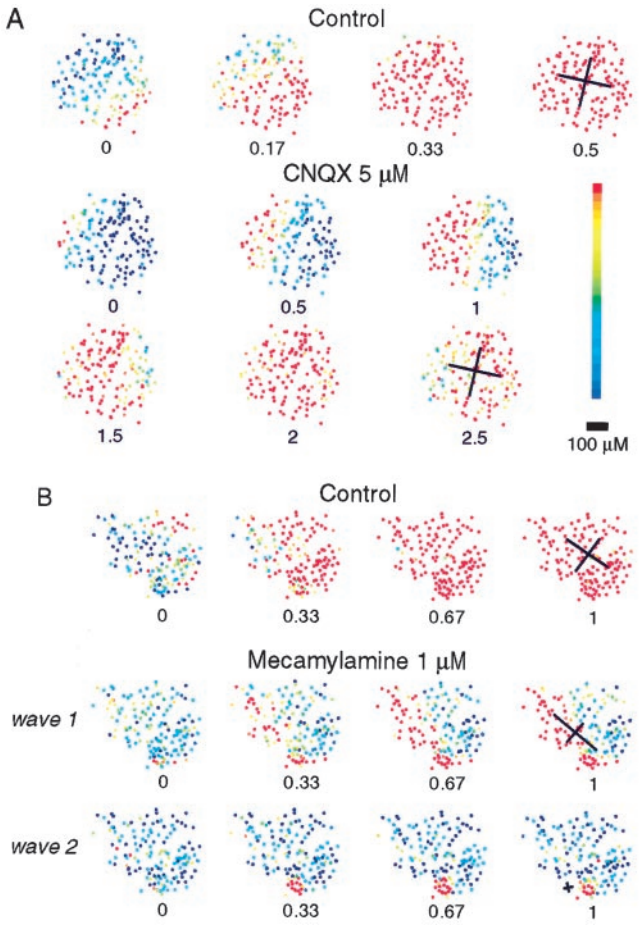

Figure 2. Different effects of glutamatergic and cholinergic blockade on wave propagation. Each *dot* represents a labeled ganglion cell. The fluorescence level of each cell is color-coded, as defined by the vertical scale bar, from *blue* for baseline levels to *red* for above-threshold activity. Each panel shows the activity at a different time (in seconds) during a wave. The *cross* shows the first-order moments at the end of each wave. It is positioned at the center of the wave (for clarity, the *small cross* for the second mecamylamine wave was drawn on the left side of the wave); the length of each long (or short) arm of the cross represents the parallel (or perpendicular) first-order moment. *A*, A control wave (*top row*) and a wave in the presence of 5 μM CNQX (*middle* and *bottom row*). Waves are much slower in the presence of CNQX, but cellular recruitment remains high. *B*, A control wave (*top row*) and two waves in the presence of 1 μM mecamylamine (*middle* and *bottom row*). In contrast to glutamatergic blockade, cellular recruitment is low during cholinergic blockade, so that activity is sometimes restricted to isolated groups of cells (*wave 2*). Such spatially restricted activity was never observed in control conditions. Examples of waves under control and drug conditions can be viewed at http://www.anc.ed.uk/~stephen/chick-waves/.

(averaged over five consecutive frames) and smoothed using an exponential smoothing function (half-life 3.5 frames). A threshold (typically 5–8% above baseline) was set for each wave to find ROIs that exhibited SBA. The cellular recruitment of a wave was the percentage of all ROIs that went above threshold. For each recruited ROI, we calculated the onset time as the point at which the trace first exceeded 20% of its peak value. The rate of rise was calculated as the gradient of the transient from the onset point to the point at which the trace exceeded 80% of its peak value. The velocity of each wave was averaged over 10 cell pairs (sometimes fewer pairs were used when recruitment was low). Cell pairs were selected parallel to the direction of the wavefront, and velocity was calculated by dividing the difference in onset time for each cell pair by the distance between them. Velocity was not calculated for waves with no clear direction (as we sometimes observed during ACh blockade). The center of a wave for each frame was defined as the first-order moment of the positions of all the ROIs above threshold (Horn, 1986). The overall extent of each wave was also measured using first-order moments. First the dominant orientation of the position of all recruited ROIs was found (Horn, 1986). The first-order moments relative to the wave center, calculated parallel and perpendicular to the dominant orientation, were then multiplied together to estimate wave extent.

To look at activity scatter, each retina was divided into a grid (7×7, 8×8, or 9×9, depending on the cellular density; see Fig. 3*C*). Grid regions with one or zero ROI were ignored. For each region, the average fluorescence amplitude of its ROIs during a wave was calculated. If this average exceeded some threshold (usually 5–10% above baseline, set on a wave-by-wave basis), the grid region was "active." For each active grid region, we calculated the percentage of active neighboring regions. Each region could have a maximum of four neighbors, one on each side (0, 25, 50, 75, 100%). Grid regions lying at the border of the grid have at most three neighbors (0, 33.3, 66.6, 100%), and corner regions have at most two neighbors (0, 50, 100%). Histograms of the percentages of neighboring active regions were then created, pooling the 75 and 66.6% bins as well as the 33.3 and 25% bins.

RESULTS

Video-rate imaging of chick embryo retinal waves

Calcium green dextran, a membrane-impermeant Ca^{2+}-sensitive dye, was injected in the optic nerve to selectively back-label ganglion cells (O'Donovan et al., 1993). Many ganglion cells scattered across the retina (over a field of view of ~500 × 500 μm^2) exhibited strong fluorescent labeling. Our recordings were made on the central retina and near the optic nerve, where the density of labeled ganglion cells was highest.

The Ca^{2+} transients we observed during spontaneous activity were faster than those described in previous studies (Wong et al., 1995; Feller et al., 1996; Catsicas et al., 1998; Wong et al., 1998) (Fig. 1*A*), probably because we have imaged at video rates (O'Donovan et al., 1993). Sometimes we observed doublets or multiplets of activity (Fig. 1*B*). Similar recurring "minibursts" have been observed during SBA in the embryonic turtle retina (Sernagor and Grzywacz, 1995), showing that our imaging technique was capable of resolving bursts of spike activity. A wave was defined as an episode of activity that was coordinated spatially and temporally in a population of ganglion cells and did not include activity restricted to isolated cells.

Under control conditions, the frequency of spontaneous waves was 37.6 ± 6.8 (mean ± SE) per hour (at 30–32°C, 4.9 mM KCl; $n = 12$ retinas). The mean cellular recruitment (see Materials and Methods) per wave was 83.9 ± 4.4% ($n = 12$ retinas, 48 waves), and the propagation velocity was 516.3 ± 117.6 μm/sec ($n = 12$ retinas, 445 pairs of cells).

Spatiotemporal modulation of retinal waves by ACh and glutamate

When cholinergic or glutamatergic connections were blocked at relatively high drug concentrations (2–30 μM), waves were completely abolished, demonstrating that both types of connections are required for wave generation. When lower drug concentrations were used, the waves persisted but were altered. This strategy allowed us to isolate the contribution of the blocked connections to wave propagation. With both types of blockade, we observed a significant drop in wave frequency and in the amplitude and rate of rise of the Ca^{2+} transients (Table 1) (for this data set all of the p values were <0.036; paired one-tailed t test). This finding suggests that retinal ganglion cell discharge, the major determinant of somatic calcium signals (O'Donovan et al., 1993; Wong et al., 1998), was similar under both types of blockade. This indicates that the changes we have observed are unlikely to be attributable to differences in the extent of blockade.

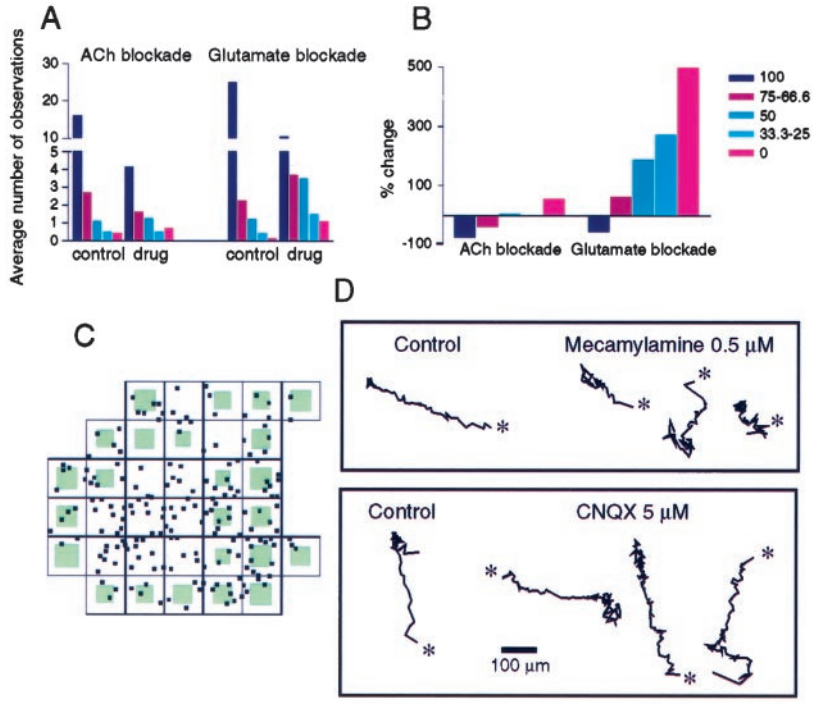

Figure 3. Cholinergic, but not glutamatergic, connections contribute to the spatial extent of the waves. *A*, Histogram showing the number of active regions surrounded by different numbers of other active regions. Each bin represents a percentage of active neighbors (see *key*). The vertical axis is broken to include the 100% bin. *B*, Percentage change in the number of active neighboring regions from control to drug blockade. *C*, Example of grid division of all ROIs in one retina during glutamatergic blockade. *Small black dots* within in each grid region indicate ROIs. *Light-gray squares* indicate active regions, with the size of the square proportional to average value of the fluorescence computed from the ROIs within the region. *D*, Trajectories of waves under different conditions. The center of each wave is drawn at each frame during a wave. *Asterisks* indicate the starting point of each wave (*bottom row*; same retina as in Fig. 2*A*).

Despite the similarities in the actions of the two types of antagonists, we found striking differences between the effects of glutamate and ACh blockade on the spatiotemporal patterns of wave propagation. During glutamate blockade, there was a substantial decrease in the velocity of wave propagation ($-33.6 \pm 9.4\%$; $p = 0.0184$, one-tailed paired t test, $n = 10$) (Fig. 2*A*) and a more modest decrease in cellular recruitment ($-17.6 \pm 4.3\%$; $p = 0.0011$, one-tailed paired t test, $n = 11$). By contrast, during ACh blockade, there was a substantial reduction in cellular recruitment with a subsequent decrease in wave spatial extent (see next paragraph for more details). Cellular recruitment was reduced by $45.1 \pm 6.7\%$ ($p = 0.0049$, one-tailed paired t test, $n = 6$), significantly more than during glutamate blockade (Table 1). Wave velocity, however, increased slightly ($+7.7 \pm 18.2\%$), and this change was not statistically significant ($p = 0.1836$, one-tailed paired t test, $n = 4$; cellular recruitment became too low for reliable velocity calculation in two additional retinas).

In contrast to glutamate antagonism, when inactive cells were scattered throughout the field of view, during cholinergic blockade the waves became spatially more restricted (Fig. 2*B*). Occasionally, the effect of cholinergic blockade on wave spread was so strong (Fig. 2*B*, *wave 2*) that the activity could not be considered as a traveling wave anymore, but rather as a cluster of coactivated cells, or bursting domain. Wave extent was quantified by looking at the first-order moments of the waves (see Materials and Methods and Fig. 2 for illustration). They dropped by 22% (20 control waves, 21 drug waves; $p = 0.0241$, Mann–Whitney U test), whereas during glutamate blockade, the drop was only 5%, which was not significant (39 control waves, 49 drug waves; $p = 0.568$, Mann–Whitney U test).

We further quantified the differences between glutamatergic and cholinergic blockade on the spatial extent of the waves using a grid analysis to compare the activity of neighboring retinal regions (see Materials and Methods). This type of analysis provides a measure of the spatial compactness of the activity across the retina. If a pharmacological treatment reduces the strength of the activity randomly across the retina, then we would expect the activity to be spatially less compact, despite still propagating across the tissue. In this case, the number of active regions surrounded by inactive regions would increase. If, on the other hand, a pharmacological treatment specifically reduces the wave spatial extent, then the remaining activity would still be compact despite propagating over a more limited area. In this case, the number of active regions surrounded by inactive regions would not increase. Figure 3*A*,*B* shows that partial glutamate blockade is associated with a decrease in the number of contiguously active regions. As shown in the histogram, under control conditions most active regions were surrounded by other active regions. After glutamate blockade, there was a significant increase in the number of active regions surrounded by inactive regions ($\chi^2 = 137.8$, $p < 0.0001$, pooled from 10 retinas; all values were normalized to the lowest number of waves used, 19 for control conditions of cholinergic blockade). In cholinergic blockade, the number of active regions was reduced, and those that remained were surrounded by other active regions ($\chi^2 = 43.8$, $p < 0.0001$, pooled from five retinas; in one retina the activity became too weak to perform the test reliably). We also compared the distributions omitting the dominant 100% bin that biases the results. In this case, glutamate but not ACh showed a significant increase in scattering ($\chi^2 = 8.00$ for glutamate, $p = 0.046$; $\chi^2 = 5.45$ for ACh, $p = 0.142$). In conclusion, cholinergic blockade, despite causing a significant drop in cellular recruitment and wave spread, did not reduce wave compactness as much as glutamatergic blockade.

These observations suggest that cholinergic connections contribute predominantly to widespread cellular recruitment, whereas glutamate influences primarily the speed of propagation. Furthermore, support for these ideas comes from examination of the trajectory of the center of the waves (Fig. 3*D*). During cholinergic blockade, the waves have a shorter and less direct trajectory, commensurate with their more restricted propagation. By contrast, during glutamate blockade the wave trajectory remains clear, despite being much slower.

DISCUSSION

This study has analyzed the excitatory synaptic circuitry underlying the spatiotemporal patterns encoded within retinal waves. Our results show, for the first time, that cholinergic and glutamatergic connections, the two main types of excitatory connections involved in retinal waves, contribute in different ways to the spatiotemporal properties of retinal SBA in the chick embryo. By recording at E14–15, we show that during the transition from early cholinergic-based activity (Catsicas et al., 1998) (E8–11) to late glutamatergic-based activity (Wong et al., 1998) (E16–18), retinal waves in the chick embryo exhibit both a glutamatergic and a cholinergic component. We suggest that these different sources of activity may play different roles during wiring of the visual system.

Glutamate modulates the temporal aspect of the waves

By regulating wave velocity, glutamate contributes significantly to the synchrony of neighboring ganglion cells, while also influencing the timing of activity between distant ganglion cells. Similar findings were reported during SBA in the embryonic turtle retina, where glutamate was found to coordinate individual spikes between neighboring ganglion cells without contributing directly to the burst propagation (Sernagor and Grzywacz, 1999).

Theoretical studies suggest that activity correlations between neighboring ganglion cells may be instructive for refining topographic maps in the central visual system (Willshaw and von der Malsburg, 1976; Eglen, 1999). We therefore speculate that glutamate may influence the refinement of retinotopic maps because changes in wave velocity will affect correlations between neighboring ganglion cells. Glutamate is also required to generate waves because high concentrations of glutamate antagonists prevent wave generation. The source of the endogenous glutamate is unknown. Synaptic sources could come from bipolar cells or from ganglion cell axon collaterals transiently present during development [discussed in Sernagor and Grzywacz (1999)]. Another possibility is that glutamate is present extracellularly, as has been reported in the developing rabbit retina (Redburn et al., 1992).

ACh modulates the spatial aspect of the waves

ACh contributes to the spatial aspect of wave propagation by ensuring cellular recruitment across broad retinal areas without exerting a substantial effect on wave velocity. By facilitating the generation of widespread cellular recruitment, ACh may influence the expansion of receptive fields and control eye-specific segregation in retinal targets. In agreement with others, we assume that cholinergic connections originate from amacrine cells (Feller et al., 1996, 1997; Sernagor and Grzywacz, 1999).

The differences between ACh and glutamate may reflect differences in the distribution of synaptic connections onto ganglion cells. Cholinergic amacrine cells have widespread dendritic arbors, allowing for connections to a large number of ganglion cells spread over a broad retinal area. Bipolar cells, on the other hand, tend to contact only a few ganglion cells over a much narrower area. Likewise, ganglion cell axon collaterals may contact only a few close neighboring cells.

As well as guiding the development of retinal axons in central targets (Shatz, 1996; Penn and Shatz, 1999), SBA also influences the development of retinal circuitry. Chronic cholinergic blockade prevents the expansion of receptive fields normally seen in dark-reared turtles (Sernagor and Grzywacz, 1996). However, high concentrations of cholinergic antagonists that abolished all SBA were used in these experiments. Hence, it is not clear whether the development of receptive fields is sensitive to a particular pattern of spontaneous activity or simply requires its presence (Crair, 1999).

During development, there is a progressive switch from cholinergic to glutamatergic synaptic transmission involved in wave generation and propagation (Wong, 1999). Accordingly, we would expect the wave spatiotemporal patterns to change from slow and widespreading to fast and spatially more restricted. In turn, this change in wave dynamics would affect the development of connectivity in the visual system. These ideas remain to be tested by theoretical and experimental investigation into the development of connectivity in the visual system, while wave patterns are chronically perturbed but not abolished. Such experiments are crucial to determine whether spontaneous activity plays an instructive or a permissive role in development.

REFERENCES

Catsicas M, Bonness V, Becker D, Mobbs P (1998) Spontaneous Ca^{2+} transients and their transmission in the developing chick retina. Curr Biol 8:283–286.

Crair MC (1999) Neuronal activity during development: permissive or instructive? Curr Opin Neurobiol 9:88–93.

Eglen SJ (1999) The role of retinal waves and synaptic normalization in retinogeniculate development. Philos Trans R Soc Lond B Biol Sci 354:497–506.

Feller MB, Wellis DP, Stellwagen D, Werblin FS, Shatz CJ (1996) Requirement for cholinergic synaptic transmission in the propagation of spontaneous retinal waves. Science 272:1182–1187.

Feller MB, Butts DA, Aaron HL, Rokhsar DS, Shatz CJ (1997) Dynamic processes shape spatiotemporal properties of retinal waves. Neuron 19:293–306.

Horn BKP (1986) Robot vision. Cambridge, MA: MIT.

Hughes WF, LaVelle A (1974) On the synaptogenic sequence in the chick retina. Anat Rec 179:297–302.

Katz LC, Shatz CJ (1996) Synaptic activity and the construction of cortical circuits. Science 274:1133–1138.

Kobayashi T, Nakamura H, Yasuda M (1990) Disturbance of refinement of retinotectal projections in chick embryos by tetrodotoxin and grayanotoxin. Dev Brain Res 57:29–35.

Maffei L, Galli-Resta L (1990) Correlation in the discharges of neighboring rat retinal ganglion cells during prenatal life. Proc Natl Acad Sci USA 87:2861–2864.

Masland RH (1977) Maturation of function in the developing rabbit retina. J Comp Neurol 175:275–286.

Meister M, Wong ROL, Baylor DA, Shatz CJ (1991) Synchronous bursts of action potentials in ganglion cells of the developing mammalian retina. Science 252:939–943.

Mey J, Thanos S (1992) Development of the visual system of the chick: a review. J Hirnforsch 33:673–702.

Miller ED, Wong WT, Wong ROL (1998) Developmental changes in the neurotransmitter regulation of correlated spontaneous retinal bursting activity. Soc Neurosci Abstr 24:812.

O'Donovan MJ, Landmesser LT (1987) The development of hindlimb motor activity studied in an isolated preparation of the chick spinal cord. J Neurosci 7:3256–3264.

O'Donovan MJ, Ho S, Sholomenko G, Yee W (1993) Real-time imaging of neurons retrogradely and anterogradely labelled with calcium-sensitive dyes. J Neurosci Methods 46:91–106.

Penn AA, Shatz CJ (1999) Brain waves and brain wiring: the role of endogenous and sensory-driven neural activity in development. Pediatr Res 45:447–458.

Penn AA, Riquelme PA, Feller MB, Shatz CJ (1998) Competition in retinogeniculate patterning driven by spontaneous activity. Science 279:2108–2112.

Pequignot Y, Clark PGH (1992a) Changes in lamination and neuronal survival in the isthmo-optic nucleus following the intraocular injection of tetrodotoxin in chick embryos. J Comp Neurol 321:336–350.

Pequignot Y, Clark PGH (1992b) Maintenance of targeting errors by isthmo-optic axons following the intraocular injection of tetrodotoxin in chick embryos. J Comp Neurol 321:351–356.

Redburn DA, Agarwal SH, Messersmith EK, Mitchell CK (1992) Development of the glutamate system in rabbit retina. Neurochem Res 17:61–66.

Sernagor E, Grzywacz NM (1995) Emergence of complex receptive field properties of ganglion cells in the developing turtle retina. J Neurophysiol 73:1355–1364.

Sernagor E, Grzywacz NM (1996) Influence of spontaneous activity and visual experience on developing retinal receptive fields. Curr Biol 6:1503–1508.

Sernagor E, Grzywacz NM (1999) Spontaneous activity in developing turtle retinal ganglion cells: pharmacological studies. J Neurosci 19:3874–3887.

Sernagor E, O'Donovan MJ (1997) Cellular mechanisms underlying retinal waves in the chick embryo. Soc Neurosci Abstr 23:306.

Shatz CJ (1996) Emergence of order in visual system development. Proc Natl Acad Sci USA 93:602–608.

Weliky M, Katz LC (1997) Disruption of orientation tuning in the visual cortex by artificially correlated neuronal activity. Nature 386:680–685.

Willshaw DJ, von der Malsburg C (1976) How patterned neural connections can be set up by self-organization. Proc Royal Soc Lond B Biol Sci 194:431–445.

Wong ROL (1999) Retinal waves and visual system development. Annu Rev Neurosci 22:29–47.

Wong ROL, Meister M, Shatz CJ (1993) Transient period of correlated bursting activity during development of the mammalian retina. Neuron 11:923–938.

Wong ROL, Chernjavsky A, Smith SJ, Shatz CJ (1995) Early functional neural networks in the developing retina. Nature 374:716–718.

Wong WT, Sanes JR, Wong ROL (1998) Developmentally regulated spontaneous activity in the embryonic chick retina. J Neurosci 18:8839–8852.